

Article

Surface Morphology of Three-Dimensionally Printed Replicas of Upper Dental Arches

Hana Eliasova ¹, Tatjana Dostalova ², Miroslav Jelinek ³, Jan Remsa ³ , Pavel Bradna ⁴,
Ales Prochazka ^{5,6}  and Magdalena Kloubcova ^{2,*}

¹ Department of Anthropology, Biology and Physiodesection, Institute of Criminalistics, Police of the Czech Republic, Strojnická 27, 170 89 Prague, Czech Republic; hanaeliasova@atlas.cz

² Department of Stomatology, 2nd Medical Faculty and Motol University Hospital, Charles University, V Uvalu 84, 150 06 Prague 5, Czech Republic; tatjana.dostalova@fnmotol.cz

³ Department of Optical and Biophysical Systems, Institute of Physics of the Czech Academy of Sciences, Na Slovance 1999/2, 182 00 Prague 8, Czech Republic; jelinek@fzu.cz (M.J.); remsa@fzu.cz (J.R.)

⁴ Department of Stomatology, 1st Faculty of Medicine, Charles University, Katerinska 32, 121 08 Prague 2, Czech Republic; pavel.bradna@vfn.cz

⁵ Czech Institute of Informatics, Robotics and Cybernetics, Czech Technical University, Jugoslavských Partyzanu 3, 160 00 Prague 6, Czech Republic; a.prochazka@ieee.org

⁶ Department of Computing and Control Engineering, University of Chemistry and Technology, Technicka 5, 166 28 Prague 6, Czech Republic

* Correspondence: magdalena.kasparova@fnmotol.cz

Received: 21 June 2020; Accepted: 12 August 2020; Published: 17 August 2020



Abstract: The aim of our study was to analyze the precision of fused-deposition modeling (FDM), polyjet technology (PJ), stereolithography (SLA) and selective laser sintering (SLS) and to evaluate some interesting indications of these methods in clinical practice. Forty upper dental arches were scanned using a 3Shape Trios 3R optical scanner system and 3D models were made. An Atos II 400 optical 3D scanner was used for calculating the coordinates of points by optical triangulation, photogrammetry and fringe projection. Each model was scanned from a minimum of 56 positions to evaluate global coordinates. Surface morphology was evaluated with an Alpha Step IQ profilometer and a JSM 5510 LV scanning electron microscope. From the measurements in cross-sections it was evident that the deviation shifted by approximately 0.1 mm. The smoothest and most homogeneous sample was SLA. SLS and SLA samples showed the most similar results in comparison of perpendicular directions (homogeneity). FDM and PJ materials exhibited significantly greater roughness in the printing direction than in the perpendicular one, which is most likely caused by the technology selected and/or print parameters. Clinical applications have demonstrated unusual treatment options for patients with rare diseases.

Keywords: orthodontics; additive manufacturing; stereolithography; fused-deposition modeling; polyjet technology; selective laser sintering; intraoral scanner

1. Introduction

Three-dimensional printing is the process of creating a 3D model of any shape from a digital model by using selective addition of material. Three-dimensional printing or rapid prototyping started in 1981, when Hideo Kodama prepared a 3D print prototype, using ultraviolet light in the process of layering of special material to construct a three-dimensional plastic model.

The term stereolithography (SLA) was used for the first time by Chuck Hull in his patent submission in 1984 (U.S. patent No. 4575330). The SLA technology is based on layer-by-layer laser beam curing of photosensitive polymers. When the layer of resin is completely polymerized, the lifting

platform moves a one-layer thickness in the vertical direction and cures the next layer and then the process is repeated many thousands of times to form a 3D physical object. The precision of printing in dentistry ranges approximately from 25 to 100 μm and printing time depends mainly on the number of layers [1].

Three-dimensional printing in dentistry and orthodontics is based mainly on intraoral scanners which contain a handheld camera, computer and software. All devices prepare a reconstruction of the dental arch with three-dimensional geometry [2]. The 3D printing result is a digital format, standard tessellation language (STL), which can be used in systems applicable in clinical practice: CEREC Omnicam (Dentsply Sirona), CEREC Bluecam (Dentsply Sirona), Planmeca Planscan (Planmeca USA), Cadent iTero (Align Technology), Carestream 3500 (Carestream Dental), 3Shape Trios 3 (3Shape North America) and 3Shape D800 model scanner (3Shape North America) [3]. The main advantages of those systems are in the data collection and treatment which is based on a virtual model and following 3D printing [4]. Trueness and precision of scanners depend also on the substrate itself and it was proved that dentin as substrate gives the most accurate scans in contrast to enamel [5]. In addition, data acquisition using an intraoral 3D scanner has shown that object rotation is an important factor which can increase or reduce distances from 0.9% to 1.4% [6].

For dentistry and orthodontics, four types of printers are the most popular: fused-deposition modeling (FDM), polyjet technology (PJ), SLA and selective laser sintering (SLS). These methods are not the only methods, where additive manufacturing plays important role. The cement-based approaches studied by Gbureck [7] with his Würzburg team aimed to develop a dual-setting biocement system based on a brushite-forming calcium phosphate cement and a tetraethyl orthosilicate based silica gel, which may be beneficial mainly in clinical applications, where we expect continuous releasing of medicaments (for example vancomycin) or support of osseointegration of implants of substances used to cure bone defects for example in maxilla-facial surgery.; De Wild with his team [8] published in 2014 research, where selective-laser-melted NiTi parts were confirmed as possible way of manufacturing of medical implants and exhibits ultra-high mechanical damping properties. The additive manufacturing using ceramic [9] and metallic materials allows to use hard materials for teeth replacement now, too.

Fused-deposition modeling (FDM) is a method of 3D printing where the final object is composed of thin layers of material which come to the printer in the form of filaments of thermoplastic material [10]. The head of the printer moves usually in one plane to create one layer of the object and is controlled digitally. As a result of this, we can usually see the layers on the surface.

Polyjet (PJ) is another kind of 3D printing technology, which uses drops of liquid photopolymer which solidify after exposure to UV light. This produces objects with a very smooth surface and thin layers of material [11].

Stereolithography (SLA) technology uses light curing of monomers, which causes polymerization and creation of a 3D object. The advantage of this method is speed of printing; the products often require machining after the priming time [10].

Selective laser sintering (SLS) uses high-power lasers to sinter powdered material to create the printed object. This can cause changes in the inner structure of the object as well as the surface.

These layers accumulate on the build tray until the part is complete. The transformation deviations during scanning from 56 positions showed that the most precise systems for surface analysis are SLA and FDM laser prints [12]. The data acquisition [13] and printing accuracy of printers depends on layer thickness which is not greater than 50 μm . The average absolute deviations for orthodontic applications must be smaller than 0.05 mm [14].

For clinical practice, the optimal size of models is equally important [15] as precise reproducibility of the surface and the shape of the dental arch in cross-section. The aim of our study was to evaluate this 3D SLA model precision in comparison with models from FDM, PJ and SLS. Our contribution aims also to evaluate the several main indications of those methods in clinical practice.

2. Materials and Methods

2.1. Three-Dimensional Prints

To check the quality of the shape of dental arches, four 3D printing techniques were used: FDM (Fortus 450 3D printer, Stratasys, Eden Prairie, MN, USA with dental SG resin) [14,16], PJ (Connex 500 3D printer, Stratasys, USA with MED 620 Resin) [17], SLS (EOSINT P 395 3D printer, EOS, USA with PA 2200 printing material based on polyamide) [18] and SLA (Form2 3D printer, Formlabs, USA with dental SG resin) [19]. The time of printing moves from 3 to 14 h. The process is directly connected on size and shape of model and its precision (from 25 μm to 100 μm). Forty upper dental arches of patients of the Department of Stomatology at Charles University and Motol University Hospital in Prague were scanned using a 3Shape Trios 3R optical scanner system. All participants were adults (20 male and 20 female) and gave their informed consent to ethical approval from the Motol University Hospital and 2nd Medical Faculty of Charles University ethics committees (EK-973IGA 1.12/11). Scanning was performed by one operator; data were stored on a computer and transferred to STL files, and all models were prepared with FDM, SLA, SLS, and PJ 3D printers following the manufacturers' directions [12].

2.2. Cross-Section Model Analysis

An Atos II 400 optical 3D scanner (GOM, Braunschweig, Germany) was used for calculating the coordinates of points by optical triangulation, photogrammetry and fringe projection. Each model was scanned from a minimum of 56 positions related to the number of teeth to define global coordinates. Transformation deviation showed precision of 3D print in the cross-section (Figure 1).

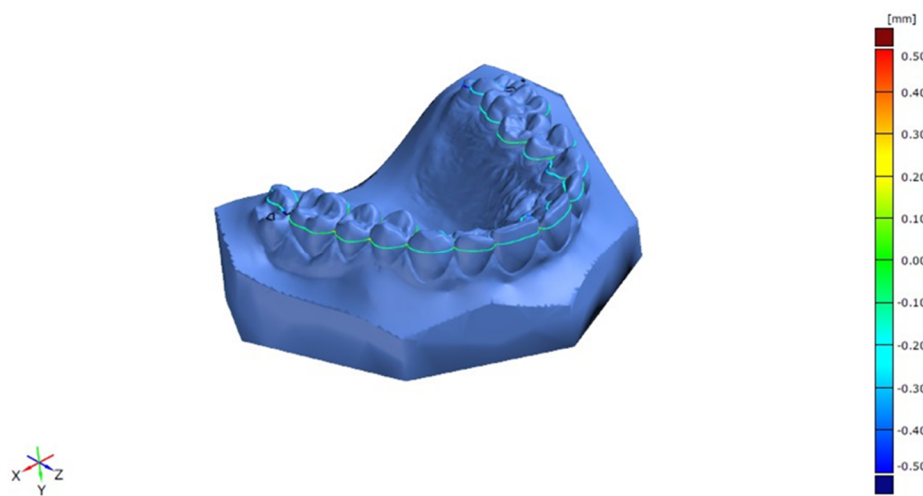


Figure 1. Digital model cross-section.

The total number of samples was forty. Every model was evaluated from 31 sectional planes, which were used for calculation of results summarized in Table 1. Two final lines of this Table were added to show means and standard deviations of these values for four printing modalities. No further calculations were done.

Table 1. Standard deviations of printed models from the nominal model created by individual printing methods (technologies) for 31 sectional planes.

	SLS	SLA	FDM	PJ
Section 1.dXYZ.1	0.000	0.039	0.226	0.000
Section 1.dXYZ.2	0.000	0.185	0.024	0.000
Section 1.dXYZ.3	0.000	0.260	0.000	0.000
Section 1.dXYZ.4	0.000	0.845	0.000	0.008
Section 1.dXYZ.5	0.000	0.396	0.000	0.001
Section 1.dXYZ.6	0.000	0.587	0.001	0.069
Section 1.dXYZ.7	0.000	0.329	0.039	0.758
Section 1.dXYZ.9	0.002	0.006	0.240	0.002
Section 1.dXYZ.10	0.002	0.008	0.004	0.000
Section 1.dXYZ.11	0.001	0.267	0.307	0.018
Section 1.dXYZ.12	0.001	0.073	0.001	0.000
Section 1.dXYZ.13	0.000	0.041	0.002	0.000
Section 1.dXYZ.14	0.001	0.162	0.000	0.000
Section 1.dXYZ.15	0.000	0.083	0.000	0.000
Section 1.dXYZ.17	0.000	0.011	0.001	0.145
Section 1.dXYZ.18	0.000	0.659	0.081	0.630
Section 1.dXYZ.19	0.000	0.654	0.226	0.206
Section 1.dXYZ.20	0.000	0.294	0.063	0.093
Section 1.dXYZ.21	0.000	0.154	0.005	0.790
Section 1.dXYZ.22	0.001	0.345	0.295	0.193
Section 1.dXYZ.23	0.011	0.837	0.171	0.034
Section 1.dXYZ.25	0.003	0.001	0.929	0.000
Section 1.dXYZ.26	0.000	0.029	1.000	0.000
Section 1.dXYZ.27	0.001	0.120	0.557	0.010
Section 1.dXYZ.28	0.000	0.004	0.000	0.000
Section 1.dXYZ.29	0.000	0.013	0.000	0.000
Section 1.dXYZ.30	0.001	0.309	0.000	0.004
Section 1.dXYZ.31	0.000	0.049	0.000	0.012
MEAN	0.001	0.241	0.149	0.106
STD	0.002	0.254	0.263	0.223

2.3. Surface and Morphology Analysis

An Alpha Step IQ profilometer (Zygo Corporation, Middlefield, CT, USA) with a scan length of 5 mm, stylus force of 14.5 μm and scan speed of 20 $\mu\text{m}/\text{s}^{-1}$ was used to analyze the profile of models. The stylus diamond tip had a 5- μm radius and 60° angle. Two places in two perpendicular directions were measured three times. Each sample was also examined under a JSM 5510 LV scanning electron microscope (Jeol, Ltd., Cambridge, UK) to show the detailed structure of the surface.

3. Results

3.1. Cross-Section Model Analysis

Processing of 3D images resulted in a cluster of points; this is further optimized to compute the polygonal mesh. This model was used for accurate analysis. Inspections were conducted in SW GOM Inspect Professional v8, software which allows advanced analysis of a 3D dimensional cluster of points obtained from the polygonal mesh produced by an optical scanner. The deviations were calculated in the form of color maps (Figure 1); this allowed the creation of inspection sections in cross-section for four printing technologies, SLS, SLA, FDM and PJ (Figure 2).

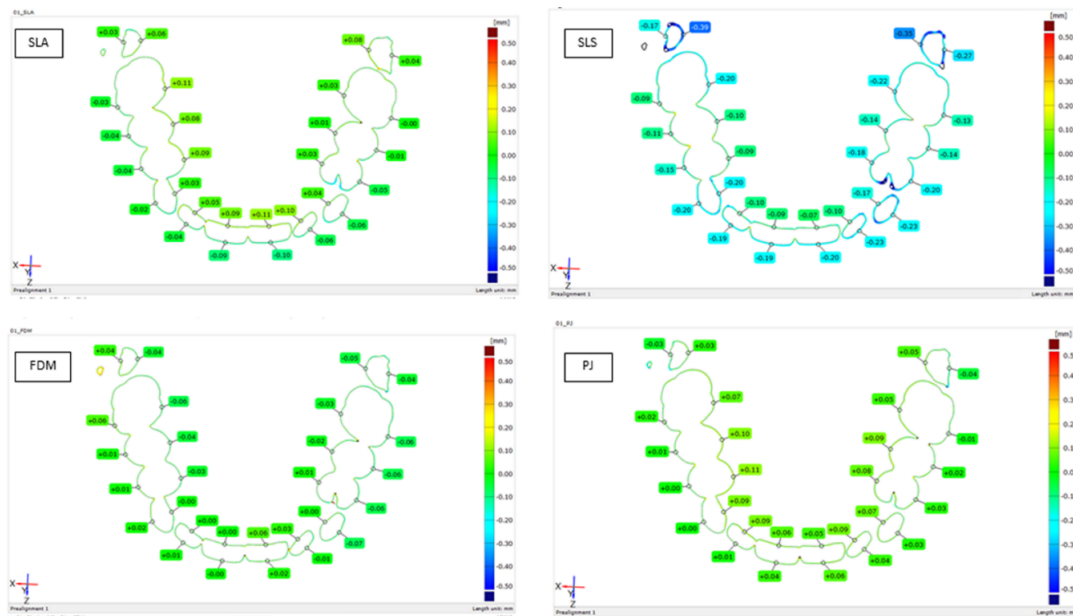


Figure 2. Precision of models in cross-section among 3D printers: stereolithography (SLA), selective laser sintering (SLS), fused-deposition modeling (FDM) and polyjet technology (PJ).

The current model was evaluated in the Cartesian coordinate system. A three-dimensional object was transformed relative to the nominal model such that the sum of squared deviations of all measured points (i.e., Cloud points) was minimal. The software calculated the perpendicular distance of each transverse point on the actual specimen from CAD data. Blue indicates measured areas that are located below the surface of the CAD (i.e., minus—less material). Red areas are located over the surface of the CAD (i.e., plus—more material). Green areas indicate no abnormalities detected. In assessing the quality of models, a color map based on the direct 2D cut was most important (Figure 2). The sectional plane passed in the same place and intersects all of the teeth in an optimal position (Table 1). In cross-section, it was evident from the measurements that the deviation shifted by approximately 0.1 mm; the accuracy was almost the same or even better than for the classical wet process [12].

3.2. Surface Structure Analysis

Surface quality is directly connected not only to the printing process, but also to different types of filament (SLA, FDM, PJ) or thermoplastic powder (SLS) (Figure 3). The FDM model showed clear lines of individual layers of the material, but at higher magnification some cuts which can influence the future durability of the material were observed. The SLS microscopic image presented a grainy structure with quite big and round grains. It was visible that this model was formed from powder. Material layering led to the creation of some holes in the structures and pits on the surface of the model. PJ material had a fibrous structure with connections of each layer. In the SLA sample, grained structures were found, but the surface was homogenous.

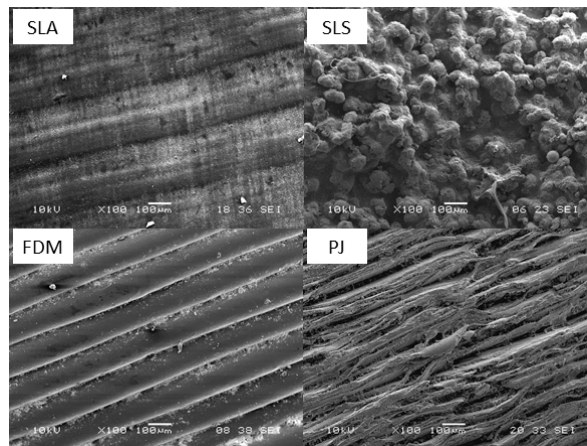


Figure 3. Surface of 3D print. (SLA) stereolithography; (SLS) selective laser sintering; (FDM) fused-deposition modeling; (PJ) polyjet technology.

Scanning electron microscope (SEM) surface analysis showed differences in the surfaces which were directly connected to the 3D printing technology and the printing material (Tables 2 and 3). The curve surface profilometry of SLA is smooth due to laser application. FDM is a method where the filaments prepare clear curves of individual layers of the material. SLS and PJ created irregular layers with small defects.

Table 2. Roughness average (Ra) measured in direction of printing.

Cutoff	Ra (nm) in Direction of Printing			
	SLA	SLS	FDM	PJ
25	0.19	0.69	1.09	1.80
80	0.65	4.30	4.78	5.35
250	1.31	10.20	8.74	12.10
800	2.37	19.35	12.80	14.00

Table 3. Roughness average (Ra) measured in direction of printing.

Cutoff	Ra (nm) Perpendicular to the Direction of Printing			
	SLA	SLS	FDM	PJ
25	0.08	1.15	0.05	0.33
80	0.31	4.10	0.33	0.63
250	1.35	10.30	0.65	4.09
800	3.66	16.95	4.33	11.45

Mechanical profilometry was utilized to determine surface roughness. The measurement took place on an Alphastep IQ device with a scan length of 5 mm, stylus force of 14.5 mg and scan speed of $20 \mu\text{m/s}^{-1}$. The stylus diamond tip has a $5\text{-}\mu\text{m}$ radius and 60° angle. Roughness average (Ra) and root mean square (Rq) values were calculated in accordance with ISO 4288, with Gaussian filters of different cutoff values (25/80/250/800 μm). To obtain reproducible results, scans were made in two places in each of two perpendicular directions (in the tooth growth/print direction and perpendicular to that) and each line was measured three times.

The smoothest and most homogeneous sample was SLA. The FDM sample was obviously printed by technology different from the others, as it was possible to observe each layer of thickness between 100 and 150 μm with the naked eye. SLS and SLA samples showed the most similar results when comparing perpendicular directions (homogeneity). FDM and PJ materials exhibited significantly

greater roughness in the printing direction than in the perpendicular one, which is most likely caused by the technology selected and/or print parameters.

3.3. SLA Clinical Application—Case Report

A 13-year-old boy with severe ID and motor delay, autism, growth delay, a high, narrow palate, widely spaced teeth, and vestibular eruption of the upper canines was referred from his dentist to the orthodontic department of the clinic (Figure 4a). This patient suffers from a rare disease—Kabuki syndrome—which is caused by a mutation in the KMT2D gene and is inherited in an autosomal dominant manner. Due to very complicated cooperation of the patient and a need for specialized orthodontic treatment of vestibular eruption of the maxillary canines, we used intraoral scanning and 3D printing to provide the patient with an appliance. Based on the treatment plan (Figure 4b), a fixed orthodontic appliance was applied in the upper jaw (Figure 4c). After 1 year of therapy, the treatment was successfully finished. The boy was not able to accept a conventional impression so an intraoral scan was prepared (Figure 4d). The digital file for the upper jaw was first converted into the STA file format (STL). The SLA 3D printer prepared a model from liquid polymer—dental SG resin (autoclavable, Class 1 biocompatible resin)—from a special resin tank during a light-based process (Figure 4e) in which the layers are polymerized by a laser beam (blue 405 nm laser). The sensor was then exposed to the laser light continuously for 5 s, and data points were recorded every 0.3 s. The laser was headed and regulated using two galvanometers. The height of one layer was 50 μm . The SLA model was completed with an orthodontic splint (Figure 4f). An orthopantomogram and photo (Figure 4g,h) were used to check the results of successful multidisciplinary therapy.

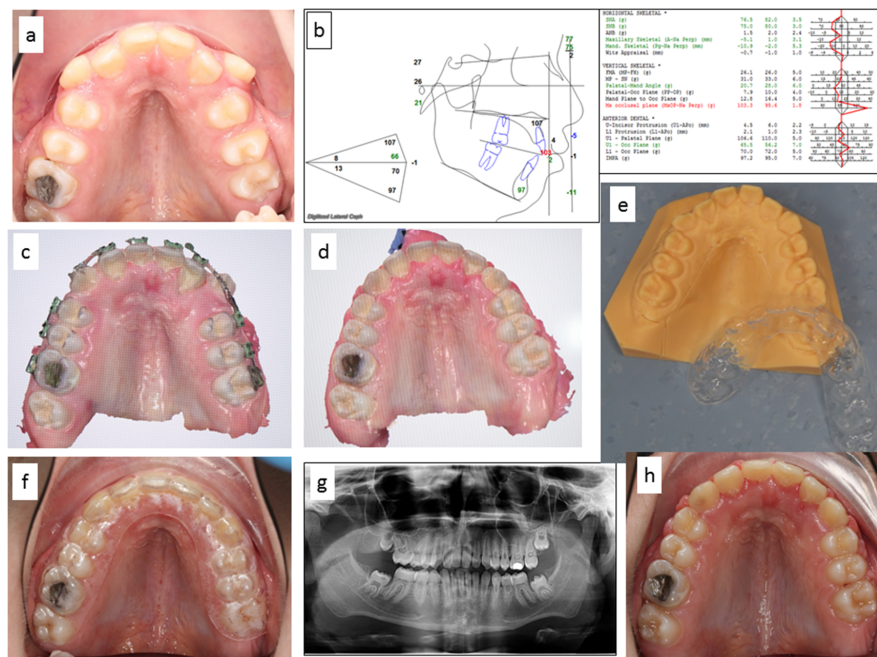


Figure 4. Orthodontic treatment based on intraoral scan and 3D print. (a) Boy with Kabuki syndrome—high, narrow palate, widely spaced teeth and vestibular eruption of the upper canines—before orthodontic therapy; (b) treatment plan; (c) intraoral scan of fixed orthodontic appliance in upper jaw; (d) intraoral 3D image of successfully finished treatment after 1 year of therapy; (e) intraoral scan converted into the stereolithography file format (STL) and 3D print SLA model from liquid polymer—dental SG resin; (f) model completed with orthodontic splint; (g,h) orthopantomogram and 2D photo after successful multidisciplinary therapy.

4. Discussion and Conclusions

Three-dimensional scanning methods associated with computational methods and modern printing technologies have many applications in stomatology and in the clinical practice now. These methods enable the examination of results of complex dental operations and corrections of dental arches as well. Associated problems are related to the accuracy of sensor systems, materials used for three-dimensional printers and the surface analysis of resulting physical models. From practical point of view, it is known that conventional impression materials provide highly accurate impressions based on highly precise plaster casts. Disadvantages of these traditional methods are the possible loss of quality due to, e.g., abrasion, attrition and transport and storage problems. On the other hand, the digital impression process using intraoral [6,15,20] scan can be resulted in loss of information. The printing is more precise, prepare long term stable material, but the time of printing is longer.

Our approach to the study used profilometer to determine surface structure of the models and electron microscope to find the inner structure. Similar approach was recently chosen by Cruz et al. to analyze surface of custom/made titanium meshes used in maxilla/facial surgery [21]. This way seems to be an alternative to micro CT scans with its pros and cons. As disadvantage we can find the necessity to destroy the examined object to characterize the inner structure. It is well known, that profilometers are great for surface analysis of 2D object, but may result in some errors in curvy objects [22]. Micro CT scans can provide information about inner and outer structure from one scan, was confirmed as useful tool in reconstruction of fine anatomic structures as for example middle ear [23], but as disadvantage we see that the method is based on X-ray, which means may have limited use in *in vivo* studies, other limitation can be also small sample size, high cost and need of specialists in the field to obtain reliable scans. Kulczyk et al. [24] published recently research comparing different methods (CT scans with standard and high resolution, optical 3D scans, micro-CT scans) of 3D data acquisition for tooth replication. Methods were examined on a dry human mandible and showed differences in quality of obtained 3D models, which may also affect 3D printing, if we use these data as source for printing. In that study authors found optical scanning better for more detailed replica than other methods mentioned.

Some studies compared various types of 3D printing with different results—surgical templates printed by the light-cured method were statistically less incongruent than those made by an FDM printer in a study by Sommacal et al. in 2015 [25]. The accuracy of models obtained by intraoral scanning is very high and shows a high level of precision even in more complicated procedures such as dental implantology and prosthodontics [26]. A study by Jang et al. from 2020 showed lower accuracy of fixed dental prostheses fabricated on a 3D printed model than on a conventional cast, but still sufficient for clinical practice [27]. Although many studies have been devoted to the accuracy of models in various clinical applications, with various results, it is not only the metric quality and stability that are important attributes of the 3D printed model: in prosthodontics, esthetic dentistry and orthodontics, the surface of the model is equally important. This also gives information about individual characteristics such as the presence and shape of mamelons, individual curves and the shape of teeth and incisal edge as well as cusps.

Specific studies are devoted to profilometer-based approach [28] and advanced micro computed tomography [29], owing to the fact that hard X-ray allow for the isotropic spatial resolution in three-dimensional space. These methods can improve possibilities of the assessment of implants and surrounding bones, to determine mineral concentration in the teeth and to estimate the thickness of enamel. In this way these methods can contribute to the appropriate use of three-dimensional models.

Intraoral scanning and 3D printing can be the only method of choice when we must take care of patients with serious diseases or handicaps where is not possible to use conventional impressions and models for dental or orthodontic treatment [30]. Wesemann et al. advise intraoral scanning in orthodontics for full arch scans but find it more time-consuming than conventional impression-taking [31]. Our case report demonstrates treatment options for a patient with a rare disease in the orofacial region with a population prevalence of less than 1:2000 inhabitants. Therapy of these

diseases is mostly long term and quality cooperation between parents and medical specialists across many different disciplines is necessary during the therapy [32]. It does not mean that the child patient cannot live a fully-fledged life with smooth integration into society in adulthood. It is necessary to take into account the limited possibility of a medically compromised patient's cooperation when devising a global therapeutic plan. Use is made of interdisciplinary cooperation with a specialized department which can give medical treatment in general anesthesia, sedation, etc. Many specialists take part in the treatment, from a geneticist to an orthodontist to a maxillofacial surgeon. The case report describes progress of the treatment of a medically compromised patient with Kabuki syndrome in our clinic. Orthodontic treatment was finished after one year and three months, with a recommendation to maintain proper hygiene by periodic check-ups of dental hygiene. The stability of therapy was supported with intraoral scans, 3D print models and special splints.

Author Contributions: Conceptualization, methodology and data validation, H.E. and T.D.; data collection, M.K., P.B.; surface and structure analysis, M.J. and J.R., Statistical analysis, final proof A.P. All authors have read and agreed to the published version of the manuscript.

Funding: This research was supported by project Ministry of Interior of Czech Republic No. VI 20152020040.

Acknowledgments: The authors thank R. Mendricky and J. Safka from the Faculty of Mechanical Engineering, Department of Production Systems and Automation, Technical University, Liberec, Czech Republic for experimental facilities.

Conflicts of Interest: No competing financial interest exist.

References

1. Duret, F.; Preston, J.D. CAD/CAM imaging in dentistry. *Curr. Opin. Dent.* **1991**, *1*, 150–154.
2. Staderini, E.; Guglielmi, F.; Cornelis, M.A.; Cattaneo, P.M. Three-dimensional prediction of roots position through cone-beam computed tomography scans-digital model superimposition: A novel method. *Orthod. Craniofac. Res.* **2019**, *22*, 16–23. [[CrossRef](#)]
3. Richert, R.; Goujat, A.; Venet, L.; Viguie, G.; Viennot, S.; Robinson, P.; Farges, J.C.; Fages, M.; Ducret, M. Intraoral scanner technologies: A review to make a successful impression. *J. Healthc. Eng.* **2017**, *2017*, 8427595. [[CrossRef](#)]
4. Staderini, E.; Patini, R.; Camodeca, A.; Guglielmi, F.; Gallenzi, P. Three-Dimensional Assessment of Morphological Changes Following Nasoalveolar Molding Therapy in Cleft Lip and Palate Patients: A Case Report. *Dent. J.* **2019**, *7*, 27. [[CrossRef](#)]
5. Bocklet, C.; Renne, W.; Mennito, A.; Bacro, T.; Latham, J.; Evans, Z.; Ludlow, M.; Kelly, A.; Nash, J. Effect of scan substrates on accuracy of 7 intraoral digital impression systems using human maxilla model. *Orthod. Craniofac. Res.* **2019**, *22* (Suppl. 1), 168–174. [[CrossRef](#)]
6. Kasparova, M.; Halamova, S.; Dostalova, T.; Prochazka, A. Intra-oral 3D scanning for the digital evaluation of dental arch parameters. *Appl. Sci.* **2018**, *8*, 1838. [[CrossRef](#)]
7. Geffers, M.; Barralet, J.E.; Groll, J.; Gbureck, U. Dual-setting brushite-silica gel cements. *Acta Biomater.* **2015**, *11*, 467–476. [[CrossRef](#)] [[PubMed](#)]
8. De Wild, M.; Meier, F.; Borman, T.; Howald, C.B.C.; Muller, B. Damping of Selective-Laser-Melted NiTi for Medical Implants. *J. Mater. Eng. Perform.* **2014**, *23*, 2614–2619. [[CrossRef](#)]
9. Diloksumpan, P.; de Ruijter, M.; Castilho, M.; Gbureck, U.; Vermonden, T.; van Weeren, P.R.; Malda, J.; Levato, R. Combining multi-scale 3D printing technologies to engineer reinforced hydrogel-ceramic interfaces. *Biofabrication* **2020**, *12*, 025014. [[CrossRef](#)] [[PubMed](#)]
10. Ngoa, T.D.; Kashania, A.; Imbalyanoa, G.; Nguzena, K.T.Q.; Huib, D. Additive manufacturing (3D printing): A review of materials, methods, applications and challenges. *Compos. Part B Eng.* **2018**, *143*, 172–196. [[CrossRef](#)]
11. Strataysys Ltd. Available online: <http://www.strataysys.com> (accessed on 20 May 2020).
12. Dostalova, T.; Kasparova, M.; Chleborad, K. Intraoral Scanner and Stereographic 3D Print in Orthodontics. In Proceedings of the SPIE Conference on Lasers in Dentistry XXV, San Francisco, CA, USA, 3 February 2019; Volume 10857.

13. Kasparova, M.; Grafova, L.; Dvorak, P.; Dostalova, T.; Prochazka, A.; Eliasova, H.; Prusa, J.; Kakawand, S. Possibility of reconstruction of dental plaster cast from 3D digital study models. *Biomed. Eng. Online* **2013**, *12*, 1–11. [CrossRef] [PubMed]
14. Zhang, Z.-C.; Li, P.-L.; Chu, F.-T.; Shen, G. Influence of the three-dimensional printing technique and printing layer thickness on model accuracy. *J. Orofac. Orthop.* **2019**, *80*, 194–204. [CrossRef] [PubMed]
15. Dostalova, T.; Kasparova, M.; Kriz, P.; Halamova, S.; Jelinek, M.; Bradna, P.; Mendricky, J. Intraoral scanner and stereographic 3D print in dentistry-quality and accuracy of model-new laser application in clinical practice. *Laser Phys.* **2018**, *28*, 125602. [CrossRef]
16. Stratasys. FDM Thermoplastics Material Overview. Available online: <http://www.stratasys.com/materials/fdm> (accessed on 6 June 2020).
17. Stratasys. Dental Molding in Digital Dentistry. Available online: <http://www.stratasys.com/materials/polyjet/dental-material> (accessed on 10 June 2020).
18. Formlabs. Professional 3D Printing Materials for Digital Dentistry. Available online: <https://formlabs.com/materials/dentistry/> (accessed on 6 June 2020).
19. Stratasys. Biocompatible Materials used in 3D Printing. Available online: <http://www.stratasys.com/materials/polyjet/bio-compatible> (accessed on 20 May 2020).
20. Prochazka, A.; Dostalova, T.; Kasparova, M.; Vysata, O.; Charvatova, H.; Sanei, S.; Marik, V. Augmented Reality Implementations in Stomatology. *Appl. Sci.* **2019**, *9*, 2929. [CrossRef]
21. Kerckhofs, G.; Pyka, G.; Moesen, M.; Van Bael, S.; Schrooten, J.; Wevers, M. High-Resolution Microfocus X-Ray Computed Tomography for 3D Surface Roughness Measurements of Additive Manufactured Porous Materials. *Adv. Eng. Mater.* **2013**, *15*, 153–158. [CrossRef]
22. Cruz, N.; Martins, M.I.; Domingos Santos, J.; Gil Mur, J.; Tondela, J.P. Surface Comparison of Three Different Commercial Custom-Made Titanium Meshes Produced by SLM for Dental Applications. *Materials* **2020**, *13*, 2177. [CrossRef]
23. Kuru, I.; Maier, H.; Müller, M.; Lenarz, T.; Lueth, T.C. A 3D-printed functioning anatomical human middle ear model. *Hear. Res.* **2016**, *340*, 204–213. [CrossRef]
24. Kulczyk, T.; Rychlik, M.; Lorkiewicz-Muszyńska, D.; Abreu-Głowacka, M.; Czajka-Jakubowska, A.; Przystańska, A. Computed Tomography versus Optical Scanning: A Comparison of Different Methods of 3D Data Acquisition for Tooth Replication. *BioMed Res. Int.* **2019**, *2019*, 4985121. [CrossRef]
25. Sommacal, B.; Savic, M.; Filippi, A.; Kühl, S.; Thieringer, F.M. Evaluation of Two 3D Printers for Guided Implant Surgery. *Int. J. Oral Maxillofac. Implant.* **2018**, *33*, 743–746. [CrossRef]
26. Matta, R.E.; Adler, W.; Wichmann, M.; Heckmann, S.M. Accuracy of impression scanning compared with stone casts of implant impressions. *J. Prosthet. Dent.* **2017**, *117*, 507–512. [CrossRef]
27. Jang, Y.; Sim, J.Y.; Park, J.K.; Kim, W.C.; Kim, H.Y.; Kim, J.H. Accuracy of 3-unit fixed dental prostheses fabricated on 3D-printed casts. *J. Prosthet. Dent.* **2020**, *123*, 135–142. [CrossRef] [PubMed]
28. Shulev, A.; Roussev, I.; Karpuzov, S.; Stoilov, G.; Ignatova, D. Roughness Measurement of Dental Materials. *J. Theor. Appl. Mech.* **2016**, *46*, 27–36. [CrossRef]
29. Erpaçal, B.; Adıgüzel, Ö.; Cangül, S. The use of micro-computed tomography in dental applications. *Int. Dent. Res.* **2019**, *9*, 78–91. [CrossRef]
30. Paderova, J.; Drabova, J.; Holubova, A.; Vlckova, M.; Havlovicova, M.; Gregorova, A.; Pourova, R.; Romankova, V.; Moslerova, V.; Geryk, J.; et al. Under the mask of Kabuki syndrome: Elucidation of genetic-and phenotypic heterogeneity in patients with Kabuki-like phenotype. *Eur. J. Med. Genet.* **2018**, *61*, 315–321. [CrossRef]
31. Wesemann, C.; Muallah, J.; Mah, J.; Bumann, A. Accuracy and efficiency of full-arch digitalization and 3D printing: A comparison between desktop model scanners, an intraoral scanner, a CBCT model scan, and stereolithographic 3D printing. *Quintessence Int.* **2017**, *48*, 41–50.
32. Staderini, E.; De Luca, M.; Candida, E. Lay People Esthetic Evaluation of Primary Surgical Repair on Three-Dimensional Images of Cleft Lip and Palate Patients. *Medicina* **2019**, *55*, 576. [CrossRef]

